1583

Compressive Failure of Single Fiber Composites

CORNELL UNIV., DEPT. OF BIOMETRICS TECHNICAL REPORT BU-1583-M

Jermaine Baldwin (University of Chicago)
Sherlyne Paret (SUNY Albany)
Carlos A. Torre (Cornell University)
S. L. Phoenix (Cornell University)

August 2001

Abstract

We present a model of a single fiber composite subject to a compressive axial load. The purpose is to better understand the origin of fiber failure as strain increases and describe the events subsequent to the initial fracture. Our model, a single fiber in a matrix, is a fourth order differential equation with a parameter in the second derivative dependant on the applied load/strain. This equation produces the oscillating solutions seen in experiments which describe the buckling phenomenon. We develop a model in order to show critical buckling failure effects, critical loads, and shape the fiber takes when fracture occurs and load is applied.

1 Introduction

There are two types of composites: natural composites, such as wood, which are found in nature, and man-made composites composed of strong, fibrous material such as carbon or boron fibers glued together in a matrix of resin such as epoxy. The use of composite materials are essential in areas such as the automotive, aerospace and aircraft industries. Due to its industrial signifigance, there has been extensive research devoted to the explanation of the compressive strength of fiber composites. The first micro-buckling model was put forth by Rosen [1]. In his two-dimensional model, the fibers are treated as an infinite array of equi-spaced, parallel plates with an elastic matrix in between. Under compression the fibers are envisaged to displace transversely in one of two distinct periodic modes called the extension mode, and the shear mode, as shown in Figure 1. In the extension mode, adjacent fibers have sinusoidal deformation patterns 180 degrees out of phase with each other. Thus along the fibers the matrix in between is placed in alternating transverse tension and compression. In the shear mode, adjacent fibers deform in phase. Thus, the matrix in between is placed in alternating positive and negative shear in proportion to the local slope of the fiber center-line relative to the original fiber axis. Rosen theoretically derived the critical loads for each mode in terms of geometric parameters, fiber and matrix stiffness. Most models describing compressive failure, are extensions of Rosen's model.

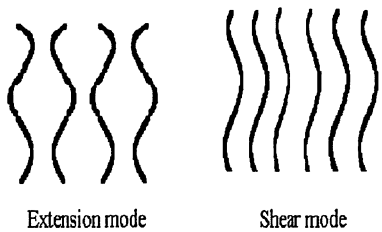

Figure 1: Two modes of fiber displacement proposed by Rosen.

In our model a single fiber is placed along the center-line of an epoxy block which is eceptionally long compared to its cross sectional diameter. The fiber is extremely strong and stiff, but its diameter is only a few microns, which is smaller than the diameter of a human hair (see Figure 2). It is evident experimentally, that occillations suddenly occur along the fiber as the applied load in the direction of the fiber is increased. Eventually, fracture occurs as a result of these occillations, which are witnessed using photo-elastic methods [7]. In order to better understand the sudden occurance of these occillations, we study the solutions of the equations derived in our model. The derived equations describe the transverse lateral displacement of the fiber as a function of the axial strain. We consider a small shear force acting on the fiber which may be caused by a slight disturbance in the matrix. For example, a bubble or particle present during the production of the fiber/matrix system that causes the fiber to become slightly off center. We consider this force to be very small in order to witness the effects of both the force and the strain on the specimen simutaineously. There are several cases that may be considered in our model. Hence, we shall discuss three cases. First, we assume the fiber has an infinite length without fracture. Second, we analyze the case of a fractured fiber of infinite length. We consider this fracture to occur at the origin for simplicity. Having a fracture at the origin represents the loss of the bending moment at this point. The photo-elastic fringe patterns suggest that the lateral displacements are extremely active at this point[7]. Finnally, we consider the situation in which the lateral strain in our model is no longer constant.

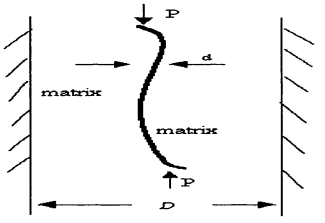

Figure 2: Single fiber in epoxy matrix.

2 Experimental and Numerical Procedures

2.1 *Equilibrium Equations for a Single Fiber Composites in Compression*

In our model we consider a single fiber composite consisting of a single cylindrical fiber of length L placed inside a cylindrical matrix such that both the fiber and the matrix have and equivalent radial axis. We define P_c as the applied compressive force. We consider the fiber, of diameter d, to be bounded on both sides by the matrix such that the effective diameter of the matrix is D, where $D \gg d$. We assume Cartesian coordinates with the fiber axis being the x-axis and the origin being midway along the fiber. We also assume the fiber has an average far field deformation per unit length, or strain ϵ_s applied to the upper and lower boundaries of the composite in the x-direction, such that the material along the the outer boundary of the matrix cylinder has a longitudinal strain ϵ_s and radial strain $-\nu_m \epsilon_s$ where ν_m is the ratio of lateral strain over axial strain, also known as the Poisson's ratio of the matrix. We let E_f be the Young's modulus, or modulus of elasticity, of the fiber. The matrix has a corresponding Young's modulus E_m as well as a shear modulus $G_m = E_m/[2(1+\nu_m)]$. We now define w as the lateral displacement of the fiber center-line, which will occur in the y-direction. Due to lateral displacements of the fiber it is possible for $0 \leq \epsilon_c \leq \epsilon_s$.

Initially we apply constant P_c along the fiber so that equilibrium in the x-direction is satisfied. There are also several other key parameters used to form our model. These parameters include Q the transverse shear force in the fiber, M the bending moment in the fiber, and σ_m and τ_m the interfacial tractions developed on the fiber surface due to transverse tension and shear in the matrix, respectively. Figure 3 represent a free-body diagram of our fiber element. As indicated in the figure, the shear tractions τ_m on the two sides of the fiber are equal but opposite in direction, whereas the transverse extensional tractions σ_m are equal and in the same direction. For the circular fiber by integrating the projected shear tractions around the fiber circumference, the couple per unit length generated is $\tau_m \pi d^2/4$ as shown by Hahn and Williams [2]. Thus we generally write this couple to be $\tau_m A_f$ where $A_f = \pi d^2/4$ is the fiber cross-sectional area.

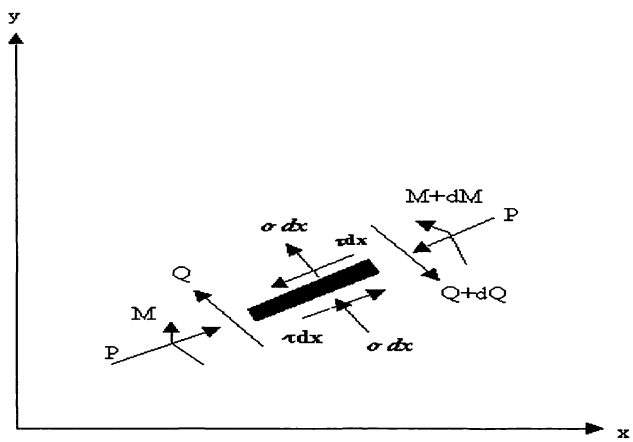

Figure 3: Free body diagram of fiber element.

As a result of our initial assumptions, the equilibrium of forces in the y-direction and moment equilibrium of the fiber element of length dx, we have

$$\frac{dQ}{dx} = 2\sigma d, \tag{1}$$

and

$$Q = \frac{dM}{dx} + P_f \frac{dw}{dx} + \tau_m A_f. \tag{2}$$

We relate σ_m and τ_m to the lateral displacements of the fiber and in a simplified approach, mimicing a 2D planar analysis as in Rosen [1].

$$\sigma_m = -2E_m \frac{w}{D-d}, \tag{3}$$

and

$$\begin{aligned} \tau_m &= -G_m(1 + \frac{d}{D-d})\frac{dw}{dx} \\ &= -G_m(\frac{D}{D-d})\frac{dw}{dx}. \end{aligned} \tag{4}$$

The term $d/(D-d)$ in (4) is an added factor which accounts approximately for the additional shear strain in the matrix caused by the finite width of the fiber when it rotates. Our initial assumption was $D \gg d$. This suggest that $d/(D-d)$ is a very small number. For this reason, it is both theoretically and experimentally essential that a suitable effective matrix diameter is chosen.

We take the bending moment in the fiber to be proportional to its local curvature [8]. Hence,

$$M = E_f I_f \frac{d^2w}{dx^2}, \tag{5}$$

where $I_f = \pi d^4/64$ is the area moment of inertia of the circular fiber about its neutral axis. Using (2),(4) and (5) the shear force Q is

$$Q = E_f I_f \frac{d^3w}{dx^3} - (B - P_f)\frac{dw}{dx} \tag{6}$$

Using our previous equations,(2),(4) and (5) we obtain the differential equation for w

$$E_f I_f \frac{d^4 w}{dx^4} - (B - P_f)\frac{d^2 w}{dx^2} + 4Kw = 0, \tag{7}$$

where

$$K = E_m \frac{d}{D-d}, \tag{8}$$

and

$$B = G_m A_f \frac{d}{D-d}, \tag{9}$$

Applying the substitutions $W = w/d$ and $\xi = x/d$ we obtain the dimensionless version of (7).

$$\frac{d^4 W}{d\xi^4} - (4\alpha - 16\epsilon_c)\frac{d^2 W}{d\xi^2} + 4\phi W = 0, \tag{10}$$

where

$$\epsilon_c = \frac{P_f}{E_f A_f}, \tag{11}$$

$$\alpha = 4\frac{B}{E_f A_f} = 4\frac{G_m}{E_f}\frac{D}{D-d}, \tag{12}$$

and

$$\phi = \frac{64K}{E_f \pi} = \frac{64 E_m d}{E_f \pi (D-d)}, \tag{13}$$

The shear modulus of the matrix provides us with the relationship between α and ϕ

$$\alpha = 4\frac{\pi}{32(1+\nu_m)}\frac{D}{d}\phi. \tag{14}$$

Our dimensionless differential equation suggests that a modified strain, which normalizes shear effects will be useful computationally. We define this revised strain β as

$$\beta = \epsilon_c - \frac{\alpha}{4}. \tag{15}$$

Now our fourth order differential equation becomes

$$\frac{d^4W}{d\xi^4} + 16\beta\frac{d^2W}{d\xi^2} + 4\phi W = 0. \tag{16}$$

The dimensionless fiber shear load S and bending moment Ω are defined as

$$S = \frac{Qd^2}{E_f I_f}, \tag{17}$$

and

$$\Omega = \frac{Md}{E_f I_f}. \tag{18}$$

Using our redefined parameter β and (5) and (6) we have

$$S = \frac{d^3W}{d\xi^3} + 16\beta\frac{dW}{d\xi}, \tag{19}$$

and

$$\Omega = \frac{d^2W}{d\xi^2}. \tag{20}$$

Now that we have formed our fourth order differential equation we use a trail solution of the form $W(\xi) = C\exp(s\xi)$ which leads to the characteristic equation

$$s^4 + \beta s^2 + 4\phi = 0. \tag{21}$$

For the fiber compressive strain range $0 \leq \beta \leq \sqrt{\phi}/4$, we factor (21) to yield

$$\left[s^2 + 8\beta\left(1 + i\sqrt{\frac{\phi}{16\beta^2} - 1}\right)\right]\left[s^2 + 8\beta\left(1 - i\sqrt{\frac{\phi}{16\beta^2} - 1}\right)\right] = 0 \quad (22)$$

In (20) we have both exponential and sinusoidal parts between the values 0 and $\frac{\sqrt{\phi}}{4}$. When $\beta = \frac{\sqrt{\phi}}{4}$ we have complex solutions and hence total sinusoidal reaction. We now notice that this equation can be rearranged to produce a general solution of the form.

$$\begin{aligned} W &= C_1 \exp -\theta_1(\beta)\xi \cos\theta_2(\beta)\xi \\ &+ C_2 \exp -\theta_1(\beta)\xi \sin\theta_2(\beta)\xi \\ &+ C_3 \exp \theta_1(\beta)\xi \cos\theta_2(\beta)\xi \\ &+ C_4 \exp \theta_1(\beta)\xi \sin\theta_2(\beta)\xi \end{aligned} \quad (23)$$

3 Graphical Analysis

Our general solution has four terms: two exponentionally decaying terms and two exponetionally increasing terms. Here, we will use the exponetionally decaying terms because of there physical signifigance.

Case 1: For this case we assume we have a fiber without fracture. The fiber is loaded and has a certain value of strain. We set the first derivative of the general solution, the slope, to zero. We consider a point ξ along the fiber disturbed by a small shear force S. Given these initial conditions we are able to plot the lateral displacement as a function of strain.

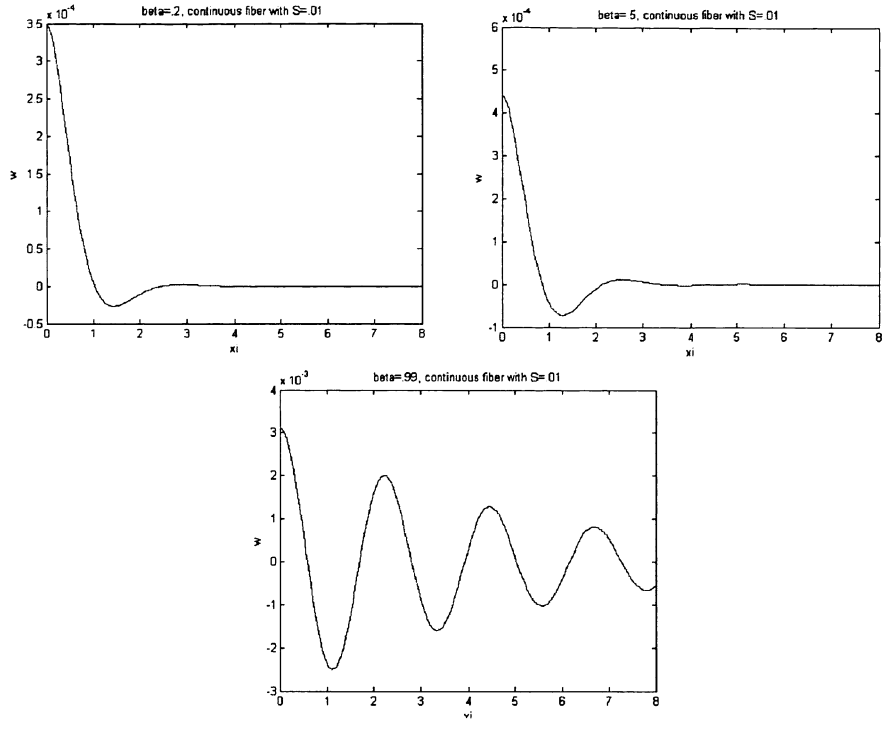

Figure 4: Graph of fiber without initial fracture

The graphs above represent the displacement of the fiber as we increase strain. As defined previously our values of strain lie on the interval $0 \leq \beta \leq \sqrt{\phi}/4$, in our case this interval is $0 \leq \beta \leq 1$. Here we notice as strain increases the displacements shift from acting as mostly exponential decay into sinusoidal.

Case 2: The difference in the next set up is that the moment is assumed to be zero, meaning that the fiber is broken at position ξ. At this fracture point, we also disturb the fiber laterally, and a solution is generated. The closer we are to zero (not much load), the exponential part of the solution dominates, and the graph decays quickly. As the load is increased, the oscillatory parts become more significant in the decaying solution.

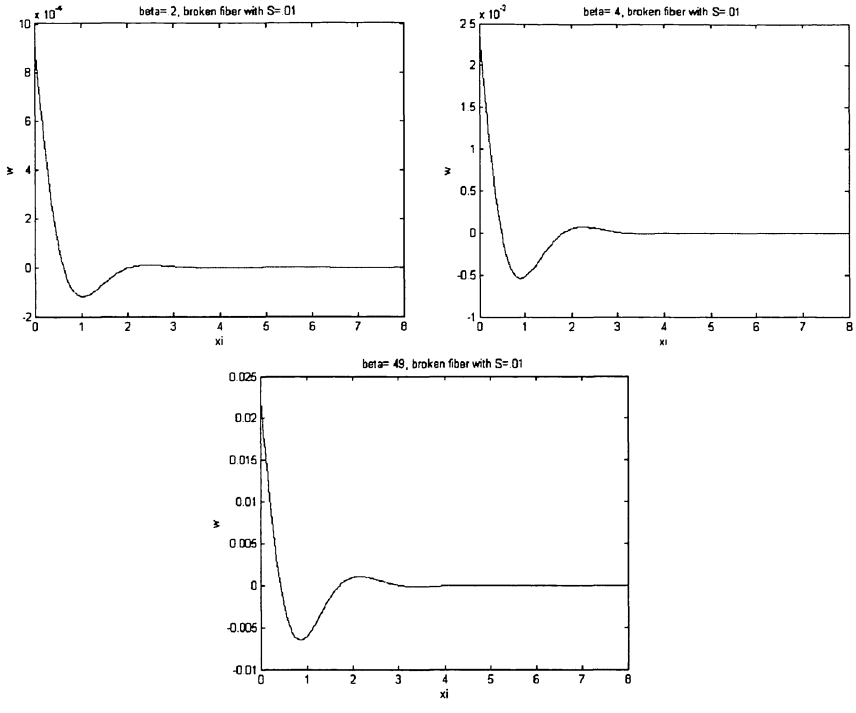

Figure 5: Graph of fiber reaction with initial fracture

When our value reaches about $\frac{\beta}{2}$ we notice that there is a sub-critical load in the fiber. Here, we apply load to the fiber in one lateral direction and it explodes to an very large value in the opposite direction. This is a result of having a fiber with some initial fracture.

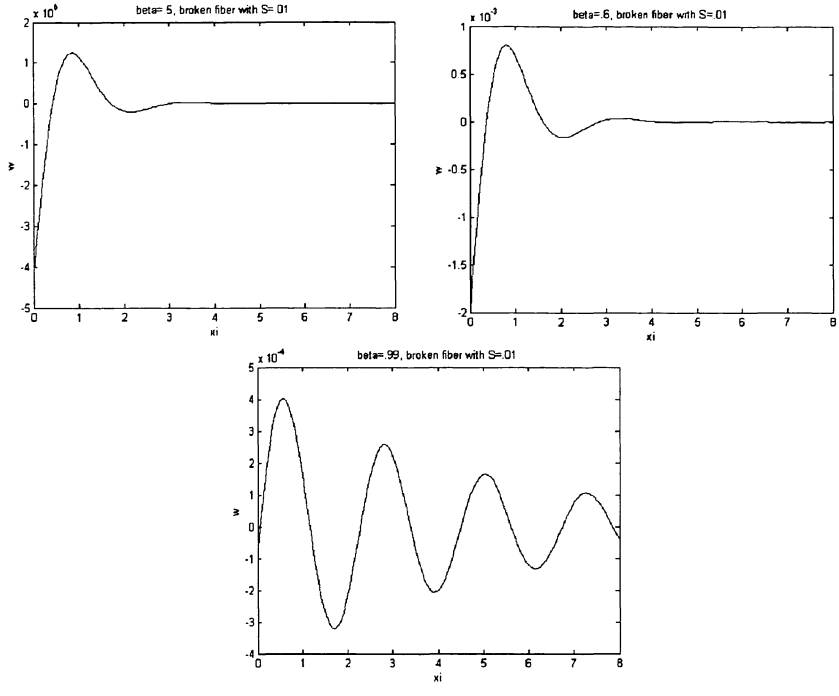

Figure 6: Graphs of sub-critical load and point thereafter.

4 Improvement to the Original Model

In all our previous cases, we assume that the strain is uniform throughout the fiber. What actually happens is a loss of strain at the point of fracture, and the recovery of strain as you move away from the fracture. This is due to an overlap in fibers at the point of fracture, which decreases the amount strain locally. Figure (?) represents a model that depicts this situation.

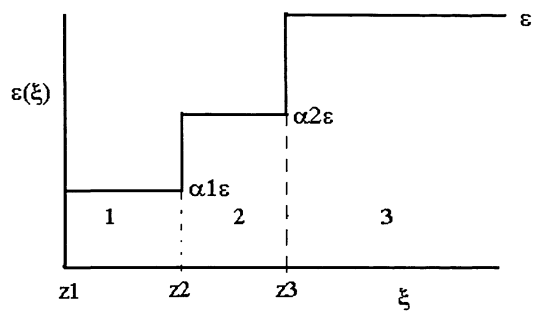

Figure 7: Strain recovery

$$\begin{aligned} W1(\xi) &\rightarrow z1 < \xi < z2 \\ W2(\xi) &\rightarrow z2 < \xi < z3 \\ W3(\xi) &\rightarrow z3 < \xi < \infty. \end{aligned}$$

Here we have 3 steps where the strain gradually increases along the ksi axis. By coupling the solutions $W1, W2, W3$, we can derive an equation that can account for the loss in strain. W1 has four constants, W2 has four constants, and W3 has only two constants, since we are only looking at the decaying part of the general solution. In order to solve for these ten constants we can come up with 10 equations by using the properties of the fiber. First position $z1$ is where the fiber is broken, and the disturbance is placed. This gives us two equations. At points $z1$ and $z2$, the position, slope, moment and shear of both solutions are equal at the defined positions: $z2 : w1 = w2, w1' = w2', w1'' = w2'', S1 = S2$ at $z3 : w2 = w3, w2' = w3', w2'' = w3'', S2 = S3$. These properties allow us to solve for the constants to get a solution to our model. It is noted that many experimental models can be derived from this setup. First, the values of $\alpha 1$ and $\alpha 2$ can be varied. Depending on their values, the recovery of strain can be linear or exponential. Also, the amount of steps and the distance between the steps can be varied to get a more precise solution.

5 Conclusion

From our analysis, it is observed that a break in the fiber affects the amount of load it can handle. This is clearly seen in the appearance of a sub-critical strain that is half the critical strain. If the strain had gone below the sub-critical point, the fiber can only handle half the load that it originally could. When the fiber breaks, there is a loss in strain at that point, and the amount of loss is extremely significant. Our developing model accounts for the local decrease of strain and can eventually improve our initial model. What we mean by improving is that the mathematical results will become more similar to the experimental results.

6 Acknowledgements

The Mathematical and Theoretical Biology Institute Research Program for Undergraduates was supported by the following grants: National Science Foundation (NSF Grant # DMS-9977919); National Security Agency (NSA Grant # MDA 904-00-1-0006; The Sloan Foundation: Cornell-Sloan National Pipeline Program in the Mathematical Sciences; Office of the Provost, Cornell University.
We would like to thank Carlos Castillo-Chavez for his support and understanding. Special thanks to S. L. Phoenix for his guidance and advice throughout this project. Mason Porter for his input and support. To Joseph and Kbenesh for all their help and moral support, much love.

References

[1] Rosen B.W.. Mechanics of Composite Strengthening. *Fiber Composite Materials,* pp. 37-75. American Society for Metals, Metals Park, Ohio(1965).

[2] Hahn H.T. and Williams J.G., *"Compression Failure Mechanisms in Unidirectional Composites,"* NASA TM 85834 (1984).

[3] Donnet J.B., and Bansal R.C. *Carbon Fibers,* Marcel Dekker Inc., New York (1990).

[4] Zheng Zeyu. Thesis. *Analytical Study of the Effect of Multiple Fiber Defects upon the Compressive Strength of Unidirectional Fiber Composites.* Cornell University, Ithaca, New York (2001).

[5] Papers from: The 1994 International Mechanical Engineering Congress and Exposion. *Buckling and Postbuckling of Composite Structure,* The American Society of Mechanical Engineers, New York, New York (1994).

[6] Ahmed K. Noor. *Buckling and Postbuckling of Composite Structure,* The American Society of Mechanical Engineers, New York, New York 1994).

[7] Deborah Schorr. Thesis. *Compressive Failure Mechanisms of Single Filament Carbon Fiber Reinforced Composites.* Cornell University, Ithaca, New York (2001).

[8] Beer F. P., and Johnson, Jr. E. R. *Mechanics of Materials.* Second Edition. New York (1992).